



Research article

Modulation of GPER1 alleviates early brain injury via inhibition of A1 reactive astrocytes activation after intracerebral hemorrhage in mice

Jianchao Mao^{a,b}, Yongkun Guo^a, Huanhuan Li^b, Hongfei Ge^b, Chao Zhang^b, Hua Feng^b, Jun Zhong^{b,*}, Rong Hu^{b,**}, Xinjun Wang^{a,***}

^a Department of Neurosurgery, The Fifth Affiliated Hospital of Zhengzhou University, Zhengzhou University, Zhengzhou, 450052, China

^b Department of Neurosurgery, Southwest Hospital, The Third Military Medical University (Army Medical University), Chongqing, 400038, China

ARTICLE INFO

Keywords:

Intracerebral hemorrhage
Early brain injury
A1 reactive astrocyte
G-protein coupled estrogen receptor 1
Toll-like receptor 4

ABSTRACT

Background: Early brain injury (EBI) caused by inflammatory responses in acute phase of Intracerebral hemorrhage (ICH) plays a vital role in the pathological progression of ICH. Increasing evidences demonstrate A1 reactive astrocytes are associated with the severity of EBI. G-protein coupled estrogen receptor 1 (GPER1) has been proved mediating the neuroprotective effects of estrogen in central nervous system (CNS) disease. However, whether GPER1 plays a protective effect on ICH and A1 reactive astrocytes activation is not well studied.

Methods: ICH model was established by infused the autologous whole blood into the right basal ganglia in wild type and GPER1 knockout mice. GPER1 specific agonist G1 and antagonist G15 were administered by intraperitoneal injection at 1 h or 0.5 h after ICH. Neurological function was detected on day 1 and day 3 by open field test and corner turn test following ICH. Besides, A1 reactive astrocytes were determined by immunofluorescence staining after ICH on day 3. To further identify the possible mechanism of GPER1 mediated neuroprotective effect, Western blot assays was performed after ICH on day 3.

Results: After ICH, G1 treatment alleviated mice neurobehavior deficits on day 1 and day 3. Meanwhile, G1 treatment also significantly reduced the GFAP positive astrocytes and the C3 positive cells after ICH. Interestingly, G15 reversed the protective effect of G1 on the neurobehavior of ICH mice. Meanwhile, the expression of GFAP⁺C3⁺ A1 reactive astrocytes were also reduced by activation of GPER1. Mechanistic studies indicated TLR4 and NF-κB mediated the neuroprotective effect of GPER1.

Conclusion: Generally, activation of GPER1 alleviated the EBI through inhibiting A1 reactive astrocytes activation via TLR4/NF-κB pathway after ICH in mice. Additionally, GPER1 may be a promising target for ICH treatment.

* Corresponding author.

** Corresponding author.

*** Corresponding author.

E-mail addresses: 1062845919@qq.com (J. Zhong), huchrong@tmmu.edu.cn (R. Hu), wangxj@zzu.edu.cn (X. Wang).

1. Introduction

Intracerebral hemorrhage (ICH) is a devastating subtype of stroke with high rates of morbidity, mortality and disability. In 2019, about 3.41 million people suffered from ICH worldwide and more than 2.89 million people died from ICH [1]. Blood is released into brain parenchyma after cerebral blood vessels ruptured, and hematoma formation compresses the surrounding normal brain tissues resulting in increased intracranial pressure, which is deemed to be primary brain injury of ICH [2]. The lysis of hematoma induces the release of blood components and erythrocyte degradation products into parenchyma which contribute to secondary brain injury (SBI) [2,3]. In the early stage of the ICH, released inflammatory factors (6–24 h) recruit more inflammatory cells, such as microglia and astrocytes (peak within 72 h post ICH) which produce more inflammatory factors, this pathological process named inflammatory cascade [4,5]. These excessive neuroinflammatory responses are one of the crucial factors for ICH leading to early brain injury (EBI) which are characterized by brain edema, reactive oxygen stress, blood-brain barrier (BBB) disruption, neuronal apoptosis and consequently neurological dysfunction [6–8]. Therefore, exploring strategies targeting inflammatory cells and excessive inflammatory response has become a focus for the treatment of ICH-induced EBI.

Astrocytes are the most abundant support cells in the central nervous system (CNS), and they play a crucial role in maintaining CNS homeostasis, for example, regulation of neurotransmitter concentrations, BBB integrity, and secreting neurotrophic factors [9–11]. After CNS suffering from insults, astrocytes are activated, proliferated and transformed into reactive astrocytes. Recent studies indicate, similar to microglia, reactive astrocytes also could be divided into two kinds of opposite phenotypes according to their morphology and function, namely, A1 and A2 reactive astrocytes [12]. The A1 reactive astrocytes produce pro-inflammatory factors and neurotoxins to induce neuronal death, whereas the A2 reactive astrocytes produce anti-inflammatory cytokines, protect CNS from the spreading neuroinflammation [13,14]. Increasing evidence verifies that A1 reactive astrocytes play a pivotal role in producing inflammatory factors after amyotrophic lateral sclerosis (ALS), ischemic stroke and traumatic spinal cord injury [15–17], suggesting that A1 reactive astrocytes are highly associated with neuroinflammation. Importantly, most recent researches demonstrate that A1 reactive astrocyte activation mediates the inflammatory response and causes early brain injury (EBI) after ICH. Inhibition of A1 reactive astrocyte activation decreases the expression of pro-inflammatory factors, reduces oxidative stress and neuronal apoptosis, and subsequently improves neurological function in ICH animals [18–20]. Herein, the inhibition of A1 reactive astrocyte activation could be a potential target for the therapy of EBI caused by ICH.

GPER1 (G-protein coupled estrogen receptor 1), also named as GPR30 is a membrane estrogen receptor, which mediates the rapid non-genomic effect of estrogen [21]. A large number of studies indicate that activation of GPER1 alleviates inflammatory responses and neurological deficits in CNS disease [22–24]. Activation of GPER1 reduces neuronal apoptosis and improves neuroprotection in subarachnoid hemorrhagic rats [25]. Additionally, a recent study has demonstrated that GPER1 participates in the regulation of astrocyte autophagy after ischemic stroke [26]. However, the effects of GPER1 on the protection of ICH-induced EBI and the mechanism underlying A1 reactive astrocyte activation after ICH have not been fully investigated.

Therefore, in the present study, we aimed to investigate the effect of GPER1 on the protection of ICH-induced EBI, and identify the role of GPER1 in the regulation of A1 reactive astrocyte activation as well as the potential molecular mechanism in ICH mice.

2. Materials and methods

2.1. Animals

A total of 89 C57BL/6J wild type (WT) mice and 19 GPER1 knockout (KO) mice (male, 22–25g, 8–10 weeks) were used in this study, and 9 WT mice, 3 GPER1 KO mice were dead before sacrifice. C57BL/6J WT mice were purchased from Byrness Weil biotech Ltd (Chongqing, China) and GPER1 KO mice were purchased from Gempharmatech Co., Ltd (Nanjing, Jiangsu, China). Mice were housed in a controlled environment at 22–25 °C, 60 ± 10% humidity, with a 12-h light/dark cycle and had free access to water and food.

2.2. Establishment of ICH model

Mice ICH model was established as our previous report [27]. In brief, the animals were anesthetized with 2% isoflurane/air mixture (2–3L/min) and fixed on stereotaxic equipment (RWD, Shenzhen, China). A total of 25 µl autologous whole blood obtained from the mouse tail was infused into the right basal ganglia (0.5 mm anterior, 2.2 mm lateral and 3.5 mm ventral) using a sterile Hamilton syringe (Imboden, Canton, Switzerland) by a micro-infusion pump (RWD, Shenzhen, China) at a speed of 2 µl/min. The infusion needle was remained in the position for at least 10 min after the blood injection was finished to prevent reflux and then the needle was gently withdrawn. The burr hole was filled with bone wax and the incision was sutured. Body temperature of mice was maintained at 37 ± 0.3 °C with a feedback-controlled heating system (Zhongshi, Inc., Beijing, China). Then, the mice were kept in a 37 °C cage for recovering from anesthesia. Sham group mice underwent the same operation procedures without infusion of blood.

2.3. Experiment design and groups

2.3.1. Experiment I: the effect of G1 on ICH mice neurofunction

To optimize the minimal effective dosage of GPER1 specific agonist G1 in the mice ICH model, 100 µg/kg and 200 µg/kg G1 (Cayman Chemical, MI, USA) were used in experiment I. A total of 32 mice were randomly divided into four groups: Sham, ICH + vehicle, ICH +100 µg/kg G1, ICH +200 µg/kg G1, n = 8 for each group. Mice received corresponding dosage G1 treatment or vehicle

after ICH model was established at 1 h. The neurological function of mice was assessed on day 1 and day 3 by open field test and corner turn test. After behavior tests, mice were sacrificed and the expression of GFAP and complement C3 in perihematomal zone were examined by western blots and immunofluorescence staining (Fig. 1A).

2.3.2. Experiment II: G15 abrogated the effect of G1

To examine whether GPER1 mediates the neuroprotective effect of G1 on ICH mice, G15, the specific antagonist of GPER1 was used to block GPER1. A total of 32 mice were randomly assigned into four groups: Sham, ICH + vehicle, ICH + G1, ICH + G1 + G15, n = 8 for each group. Mice received 200 µg/kg G15 (Cayman Chemical, MI, USA) treatment at 0.5 h, and G1 (200 µg/kg) or vehicle was given at 1 h after ICH. Neurological function was evaluated on day 1 and day 3 via open field test and corner turn test. After behavior tests, brains were collected and A1 reactive astrocytes were detected by immunofluorescence staining in perihematomal region. Meanwhile, complement C3, GFAP and the potential molecular mechanism TLR4, NF-κB were evaluated by Western blot. G1 and G15 were dissolved in DMSO (Sigma-Aldrich, St. Louis, MO, Germany) and diluted into corresponding dosage. 100 µl G1 or G15 or vehicle was administered via intraperitoneal injection (Fig. 1B).

2.3.3. Experiment III: knockout GPER1 reversed the effect of G1 on ICH mice

To further verify the effect of GPER1 on ICH mice, GPER1 KO mice were used in experiment III. A total of 16 WT mice and 16 GPER1 KO mice were randomly divided into four groups: ICH (WT) + vehicle, ICH (WT) + G1, ICH (KO) + vehicle, and ICH (KO) + G1, n = 8 in each group. Mice received G1 treatment or vehicle after ICH model was established at 1 h. And on the day 3 post-ICH, the expression of A1 reactive astrocytes was detected by immunofluorescence staining. Besides, GFAP, complement C3, TLR4 and NF-κB were evaluated by western blots in perihematomal area (Fig. 1C).

2.4. Behavior tests

2.4.1. Open field test

Open field test was performed to evaluate the spontaneous motor function of mice after ICH on day 1 and day 3. And the test procedure was performed as our previous report [27], briefly, the woody apparatus was equally divided into four quadrants with the same size and adjacent with each other but isolated (50 cm length, 50 cm width, and 50 cm height). Each mouse of different groups was placed in the same quadrant for 5 min, and the move trajectory was recorded by a camera. Then, the equipment was cleaned up by 75% alcohol to wipe the mess, and while the equipment was dry, the next animal test was performed. The video data was then analyzed by

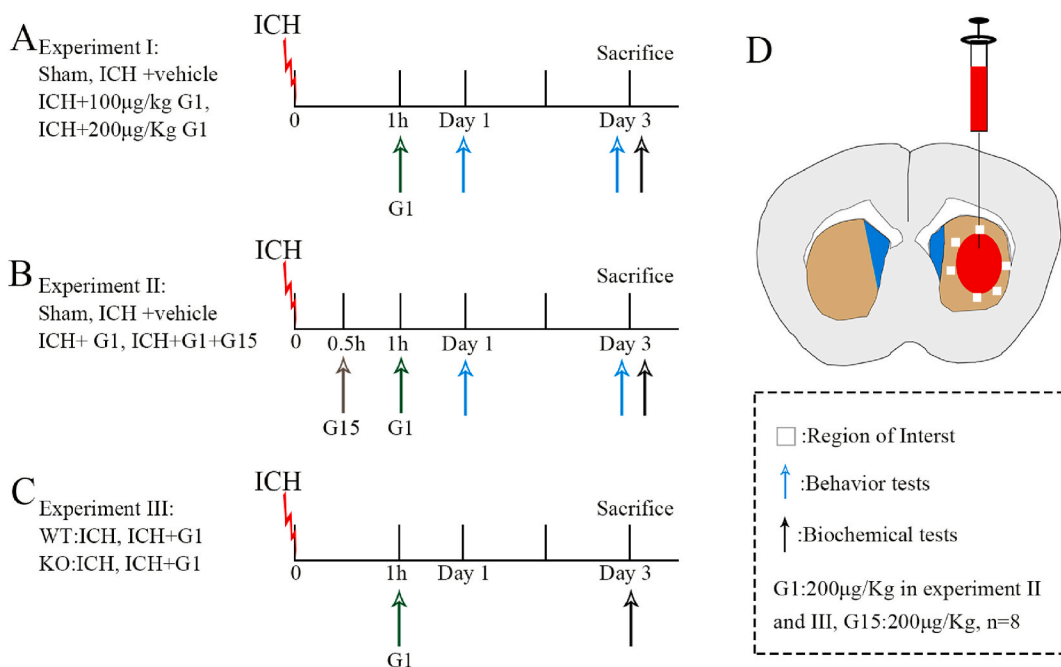


Fig. 1. Schematic diagram of experimental design and mice ICH model. (A) The groups and time course of experimental I. Behavior tests included open field test and corner turn test, n = 8 in each group. Biochemical tests included immunofluorescence staining (n = 4) and western blots (n = 4). (B) The groups and time course of experimental II. Behavior tests included open field test and corner turn test, n = 8 in each group. Biochemical tests included immunofluorescence staining (n = 4) and western blots (n = 4). (C) The groups and flowchart of experiment III. Biochemical tests included immunofluorescence staining (n = 4) and western blots (n = 4). (D) Illustration of mice ICH model and the white blanks represented the regions of interests.

two independent examiners blinded to the experimental groups to measure the total distance of free movement by using a software (ViewPoint Behaviour Technology, Lyon, France).

2.4.2. Corner turn test

The corner turn test was also performed to assess the neurological function of ICH mice. The device which consisted of two boards forming a 30° angle vertically on the platform was utilized to perform the test. The mice were allowed to step into a 30° angle corner and exit by turning either to the left or the right. Choice of turning was recorded for a total of ten trials, and the result was the percent of right turns in 10 trials. And the interval of each trial was at least 30 s.

2.5. Immunofluorescence

After behavior tests, the mice were deeply anesthetized and perfused via cardiac with ice-cold PBS and followed with 4% paraformaldehyde. Brains were collected and dehydrated using 30% sucrose solution at 4 °C for two days. Then, brains were embedded by OCT compound and coronal sections were prepared (20 μm) by freezing microtome (CM1860, Leica, IL, USA). Then, slices were incubated with 0.3% Triton X-100 (Sigma-Aldrich, St. Louis, MO, Germany) to penetrate the membranes at room temperature for 30 min. After washed with PBS for three times, samples were rinsed in 5% BSA to block the non-specific site at room temperature for 2 h. Then, samples were incubated with following primary antibodies: goat polyclonal to GFAP (1:200, Abcam, Cambridge, UK), rabbit

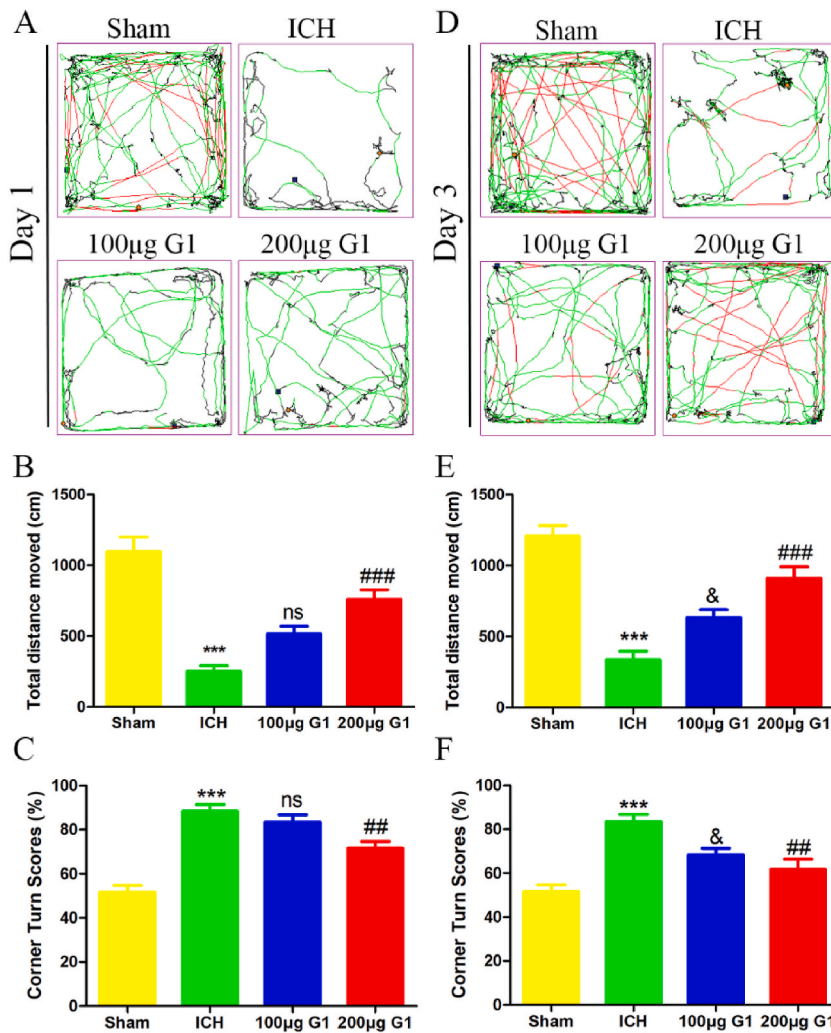


Fig. 2. G1 relieved the neurological dysfunction of ICH mice. (A) The representative movement trajectory in open field test on day 1 post-ICH. (B) Total distance moved in open field test on day 1 after ICH. (C) Corner turn test scores on day 1 after ICH. (D) Representative movement trajectory in open field test on day 3 post-ICH. (E) Total distance moved in open field test on day 3 after ICH. (F) Corner turn test scores on day 3 post-ICH. n = 8 in each group, ***p < 0.001 vs Sham group, ns indicated no significantly difference vs ICH group, &p < 0.05 vs ICH group, ##p < 0.01 vs ICH group, ###p < 0.001 vs ICH group.

polyclonal to C3 (1:100, Proteintech, Wuhan, China) at 4 °C overnight. Later, relative fluorescence-conjugated secondary antibodies (1:400, Proteintech, Wuhan, China) were incubated at room temperature for 2 h in the condition of avoiding light. DAPI (Boster, Wuhan, China) was incubated for 10 min at room temperature to counteract the nucleus. Images were captured through Carl Zeiss confocal fluorescence microscope (LSM880, Carl Zeiss, Weimar, Germany) and analyzed by Image J software (Image J 1.8, NIH, USA).

2.6. Western blots

Brain tissues around the hematoma were collected after decapitation post-ICH on day 3. The perihematoma tissues were homogenate with RIPA (Sigma-Aldrich, St. Louis, MO, Germany) and the lysates were obtained after centrifuge, and the protein concentration of each sample was determined by using a bicinchoninic acid (BCA) method (Beyotime, Shanghai, China). A total of 50 µg protein were separated by 10% SDS-PAGE under reducing conditions and transferred to polyvinylidene difluoride membranes (Merck, Darmstadt, Germany). Then, the membranes were incubated in 5% (w/v) non-fat dry milk (Beyotime, Shanghai, China) in Tris-HCl buffer solution + Tween (TBST) at room temperature for 2 h. Afterward, they were washed by TBST to remove the milk, then the membranes were cut horizontally to separate interest protein and housekeeping protein, and then they were incubated separated in mouse monoclonal to GFAP (1:1000, Abcam, Cambridge, UK), rabbit polyclonal to C3 (1:1000, Boster, Wuhan, China), rabbit polyclonal to TLR4 (1:1000, Bioss, Beijing, China), mouse monoclonal to NF-κB (1:1000, Bioss, Beijing, China), and mouse monoclonal to GAPDH (1:20000, Proteintech, Wuhan, China) as a loading control at 4 °C overnight. Then, after washed with TBST for 3 times, the membranes were incubated with relative HRP-conjugated secondary antibodies (1:5000, Boster, Wuhan, China) at room temperature for 2 h. The optic density was visualized using an imaging system (Evolution-Capt Edge, Vilber, France) with a Western blot chemiluminescence kit (Thermo Fisher Scientific, Waltham, MA, USA). Densitometric measurement of each membrane was performed using Image J software (Image J 1.8, NIH, USA).

2.7. Statistical analysis

The sample size was determined according to our previous study and other studies [20,27]. All data were presented as mean ± SEM. The statistical analyses were performed using SPSS 20.0 software (SPSS, Inc., Chicago, IL, United States). One-way analysis of variance followed by Turkey's post hoc test was used for comparisons, as appropriate. $p < 0.05$ was considered to be statistically significant.

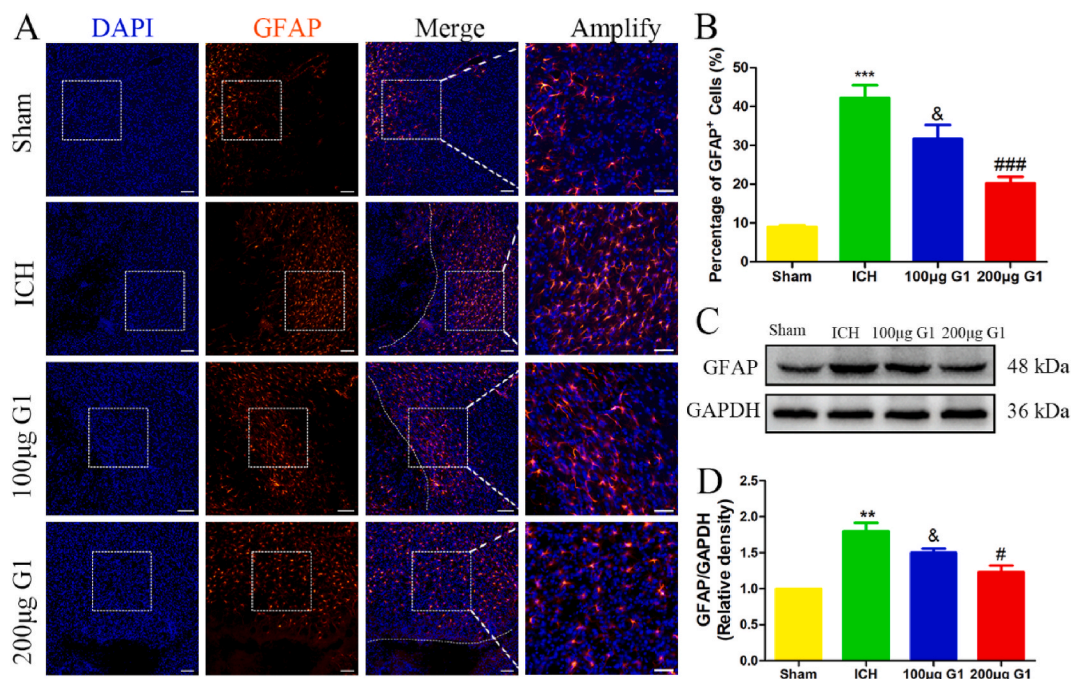


Fig. 3. G1 reduced the activation of astrocytes after ICH. (A) Representative images of GFAP (orange) staining in perihematoma region in different groups on day 3 after ICH. (B) Quantification analysis of GFAP positive cells in each group. (C) Representative bands of GFAP protein around hematoma tissues in different groups on day 3 after ICH, GAPDH was a loading control. (D) Statistical analysis of GFAP protein expression in different groups. $n = 4$ in each group, ** $p < 0.01$ vs Sham group, *** $p < 0.001$ vs Sham group, & $p < 0.05$ vs ICH group, # $p < 0.05$ vs ICH group, ### $p < 0.001$ vs ICH group. Scale bar: 50 µm.

3. Results

3.1. Activation of GPER1 using its agonist G1 mitigated neurological deficits of ICH mice

To investigate the effect of GPER1 specific agonist G1 on the neurofunction of ICH mice, we adapted the autologous blood infused method to establish the mice ICH model (Fig. 1D). The movement trajectory of open field test showed ICH decreased the movement of mice in center of the field and the total moved distance compared with Sham group on day 1 after ICH, and administration of G1 alleviated the movement impairment of ICH mice (Fig. 2A). Quantitative analyses indicated ICH decreased the total moved distance to about 22% compared with Sham group (250 ± 40.04 vs 1097 ± 102.3 cm, $p < 0.001$), and G1 increased the total moved distance compared with ICH + vehicle group significantly at 200 $\mu\text{g}/\text{kg}$ (758.8 ± 68.46 vs 250 ± 40.04 cm, $p < 0.001$, Fig. 2B). Corner turn test also suggested ICH increased the rate of right turn compared with Sham group (88.33 ± 3.073 vs $51.67 \pm 3.073\%$, $p < 0.001$), while 100 $\mu\text{g}/\text{kg}$ G1 (83.33 ± 3.333 vs $88.33 \pm 3.073\%$, $p > 0.05$), 200 $\mu\text{g}/\text{kg}$ G1 (71.67 ± 3.073 vs $88.33 \pm 3.073\%$, $p < 0.01$) decreased the rate of right turn compared with ICH + vehicle group (Fig. 2C). On the day 3 after ICH, the total moved distance in open field test still decreased compared with Sham group (336.8 ± 58.93 vs 1208 ± 72.31 cm, $p < 0.001$), and 100 $\mu\text{g}/\text{kg}$ G1 (632.6 ± 56.99 vs 336.8 ± 58.93 cm, $p < 0.05$), 200 $\mu\text{g}/\text{kg}$ G1 (909.5 ± 82.03 vs 336.8 ± 58.93 cm, $p < 0.001$) increased the total moved distance compared with ICH + vehicle group (Fig. 2D and E). Similarly, corner turn test also indicated ICH increased the rate of right turn (83.33 ± 3.333 vs $51.67 \pm 3.073\%$, $p < 0.001$) and G1 suppressed the increase of right turn caused by ICH (68.33 ± 3.073 vs $83.33 \pm 3.333\%$, $p < 0.05$, for 100 $\mu\text{g}/\text{kg}$ G1, 61.67 ± 4.773 vs $83.33 \pm 3.333\%$, $p < 0.01$, for 200 $\mu\text{g}/\text{kg}$ G1, Fig. 2F). These data suggested activation of GPER1 by administration of its specific agonist G1 mitigated the neurological deficits in ICH mice.

3.2. G1 reduced astrocytes activation and decreased the expression of C3 in ICH mice

Considering that astrocytes are proliferated and activated robustly after CNS insult, we determined the activation and proliferation of astrocytes after ICH. As shown in Fig. 3A, on day 3 after ICH, GFAP positive astrocytes proliferated rigorously in perihematomal tissues, and the administration of G1 decreased the proliferation of astrocytes. Quantification analysis demonstrated ICH increased the rate of GFAP positive astrocytes robustly (42.2 ± 3.262 vs $9 \pm 0.4472\%$, $p < 0.001$), and 100 $\mu\text{g}/\text{kg}$ G1 (31.6 ± 3.641 vs $42.2 \pm 3.262\%$, $p < 0.05$), 200 $\mu\text{g}/\text{kg}$ G1 (20.2 ± 1.655 vs $42.2 \pm 3.262\%$, $p < 0.001$) significantly decreased the rate of GFAP positive astrocytes compared to ICH + vehicle group (Fig. 3B). Western blots further suggested ICH increased the expression of GFAP protein, and G1 reversed the increase of GFAP protein (Fig. 3C). Semi-quantification analysis showed ICH increased the expression of GFAP protein to 1.8 ± 0.1155 folds ($p < 0.01$), and G1 decreased the expression of GFAP compared with ICH + vehicle group (1.5 ± 0.05774 vs 1.8 ± 0.1155 folds, for 100 $\mu\text{g}/\text{kg}$ G1, $p < 0.05$, 1.233 ± 0.08819 vs 1.8 ± 0.1155 folds, for 200 $\mu\text{g}/\text{kg}$ G1, $p < 0.05$, Fig. 3D).

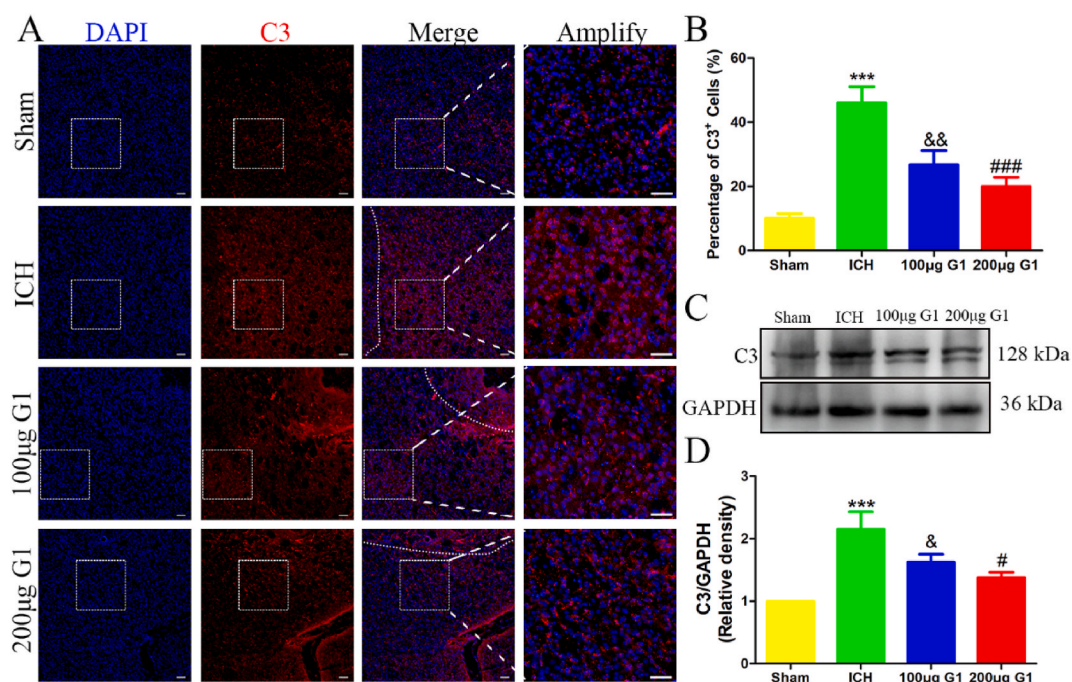


Fig. 4. G1 inhibited the expression of complement C3 post-ICH. (A) Representative images of C3 positive cells (red) in perihematoma area in different groups on day 3 after ICH. (B) Quantification analysis of C3 positive cells. (C) Representative bands of C3 in perihematoma tissues on day 3 after ICH, GAPDH as a loading control. (D) Statistical analysis of C3 protein expression. $n = 4$ in each group, *** $p < 0.001$ vs Sham group, & $p < 0.05$, && $p < 0.01$ vs ICH group, # $p < 0.05$ vs ICH group, ### $p < 0.001$ vs ICH group. Scale bar: 50 μm .

Complement C3 as a marker of A1 reactive astrocytes, it also linked with inflammatory response after CNS damage. Thus, we determined the expression of C3 after ICH. On the day 3 after ICH, C3 positive cells increased markedly in perihematomal region, and G1 partially abolished this phenomenon (Fig. 4A). Quantitative analysis indicated ICH increased the ratio of C3 positive cells significantly (46 ± 5.099 vs $10.2 \pm 1.393\%$, $p < 0.001$), and 100 $\mu\text{g}/\text{kg}$ G1 (26.8 ± 4.329 vs $46 \pm 5.099\%$, $p < 0.01$), 200 $\mu\text{g}/\text{kg}$ G1 (20 ± 2.811 vs $46 \pm 5.099\%$, $p < 0.001$) obviously decreased the ratio of C3 positive cells compared with ICH + vehicle group (Fig. 4B). Western blots also indicated the expression of C3 protein markedly increased after ICH (2.15 ± 0.2784 vs 1 folds, $p < 0.001$) compared with Sham group, and 100 $\mu\text{g}/\text{kg}$ G1 (1.625 ± 0.125 vs 2.15 ± 0.2784 folds, $p < 0.05$), 200 $\mu\text{g}/\text{kg}$ G1 (1.375 ± 0.08539 vs 2.15 ± 0.2784 folds, $p < 0.05$) reversed the expression of C3 on day 3 after ICH (Fig. 4C and D). These results manifested activation of GPER1 inhibited the activation and proliferation of astrocytes, decreased the expression of complement C3 caused by ICH and improved the neurological function in ICH mice. Due to the effective protection of 200 $\mu\text{g}/\text{kg}$ G1 on the neurological function and the inhibition of astrocyte activation. Thus, we adapted 200 $\mu\text{g}/\text{kg}$ G1 as treatment dosage in the followed experiments.

3.3. G15 abrogated the protective effects of G1 on neurological function in ICH mice

Next, we investigated whether the protective effects of G1 on neurological function of ICH mice was relied on GPER1. GPER1 specific antagonist G15 was utilized to block GPER. Open field test data showed ICH decreased the total moved distance (204.4 ± 51.41 vs 1235 ± 55.41 cm, $p < 0.001$) and administration of G1 increased the total moved distance (787.4 ± 74.28 vs 204.4 ± 51.41 cm, $p < 0.001$). However, the administration of G15 30 min prior to G1 markedly suppressed the effect of G1 on the motor function of

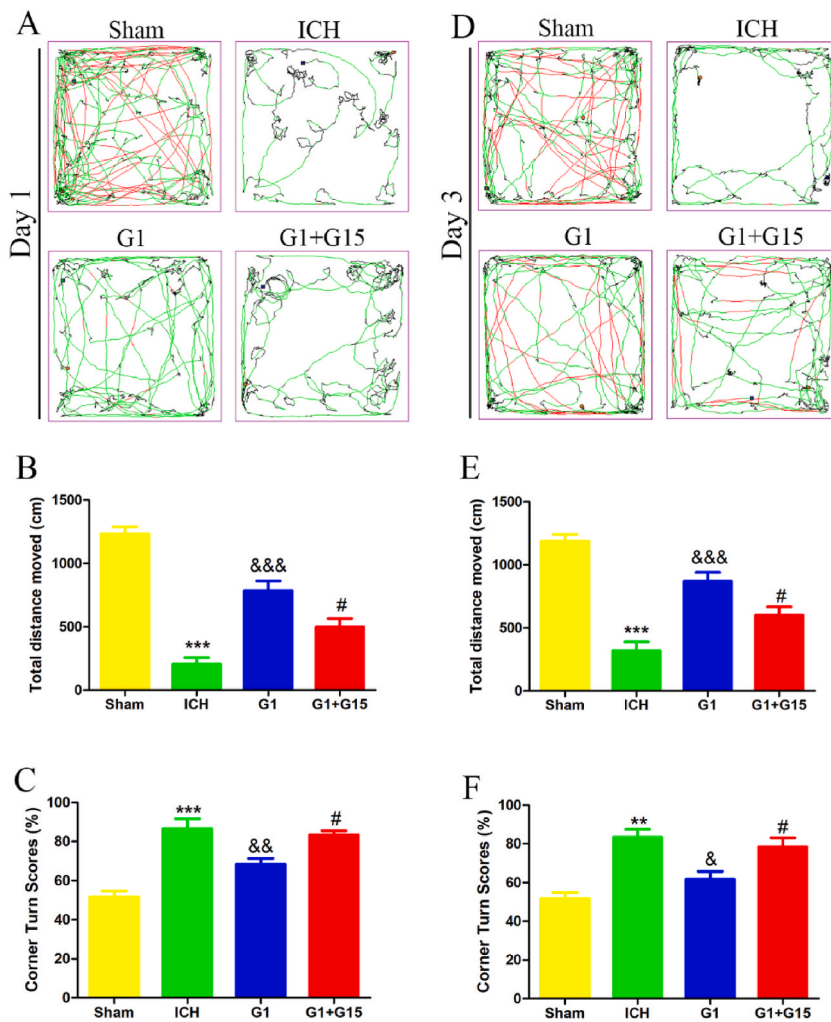


Fig. 5. G15 reversed the protective effects of G1 on neurological function in ICH mice. (A) Representative movement trajectory in open field test on day 1 after ICH. (B) Total distance moved in open field test on day 1 after ICH. (C) Corner turn test scores on day 1 after ICH. (D) Representative movement trajectory in open field test on day 3 after ICH. (E) Total distance moved in open field test on day 3 after ICH. (F) Corner turn test scores on day 3 after ICH. $n = 8$ in each group, $**p < 0.01$ vs Sham group, $***p < 0.001$ vs Sham group, $\&\&p < 0.01$ vs ICH group, $\&\&\&p < 0.001$ vs ICH group, $\#p < 0.05$ vs G1 group.

ICH mice on day 1 (500.1 ± 65.2 vs 787.4 ± 74.28 cm, $p < 0.05$, Fig. 5A and B). The corner turn test on day 1 after ICH also indicated G1 alleviated the rate of right turn compared with ICH + vehicle group (68.33 ± 3.073 vs $86.67 \pm 4.944\%$, $p < 0.01$), but G15 reduced the protective effect of G1 (83.33 ± 2.108 vs $68.33 \pm 3.073\%$, $p < 0.05$, Fig. 5C). Similar with day 1, open field test on day 3 after ICH showed G1 increased the total moved distance compared with ICH + vehicle group (870.1 ± 70.66 vs 320 ± 67.8 cm, $p < 0.001$), and G15 reduced the total moved distance (602.8 ± 63.52 vs 870.1 ± 70.66 cm, $p < 0.05$) compared with ICH + G1 group (Fig. 5. D, E). And the corner turn test also indicated G15 suppressed the protective effect of G1 on neurological function of ICH mice on day 3 (78.33 ± 4.773 vs $61.67 \pm 4.014\%$, $p < 0.05$, Fig. 5. F). These data suggested G1 protected the neurological function from ICH was in a GPER1 dependent manner.

3.4. G15 abolished the effect of G1 on inhibition of A1 reactive astrocytes in ICH mice

Due to the vital role of A1 reactive astrocytes on the inflammatory response and progression of ICH, the A1 reactive astrocytes activation after ICH was then examined. The results showed, on the day 3 after ICH, the GFAP and C3 positive cells, namely A1 reactive astrocytes, were activated rigorously compared with Sham group (41.83 ± 3.188 vs $8.667 \pm 1.406\%$, $p < 0.001$), and G1 reduced the activation of A1 reactive astrocytes compared with ICH + vehicle group (22.67 ± 2.092 vs $41.83 \pm 3.188\%$, $p < 0.001$). However, G15 mitigated the inhibition of G1 on the activation of A1 reactive astrocytes compared with ICH + G1 group (33.83 ± 2.428 vs $22.67 \pm 2.092\%$, $p < 0.05$, Fig. 6 A, B). Moreover, the western blots also showed G1 reduced, the A1 reactive astrocytes markers, GFAP (1.5 ± 0.07071 vs 2.38 ± 0.1828 folds, $p < 0.001$) and C3 (1.436 ± 0.07277 vs 2.6 ± 0.228 folds, $p < 0.001$) expression after ICH, and G15 reversed the effect of G1 on the expression of GFAP and C3 ($p < 0.01$, Fig. 6 C, D). These data indicated activation of GPER1 reduced the activation of A1 reactive astrocytes after ICH.

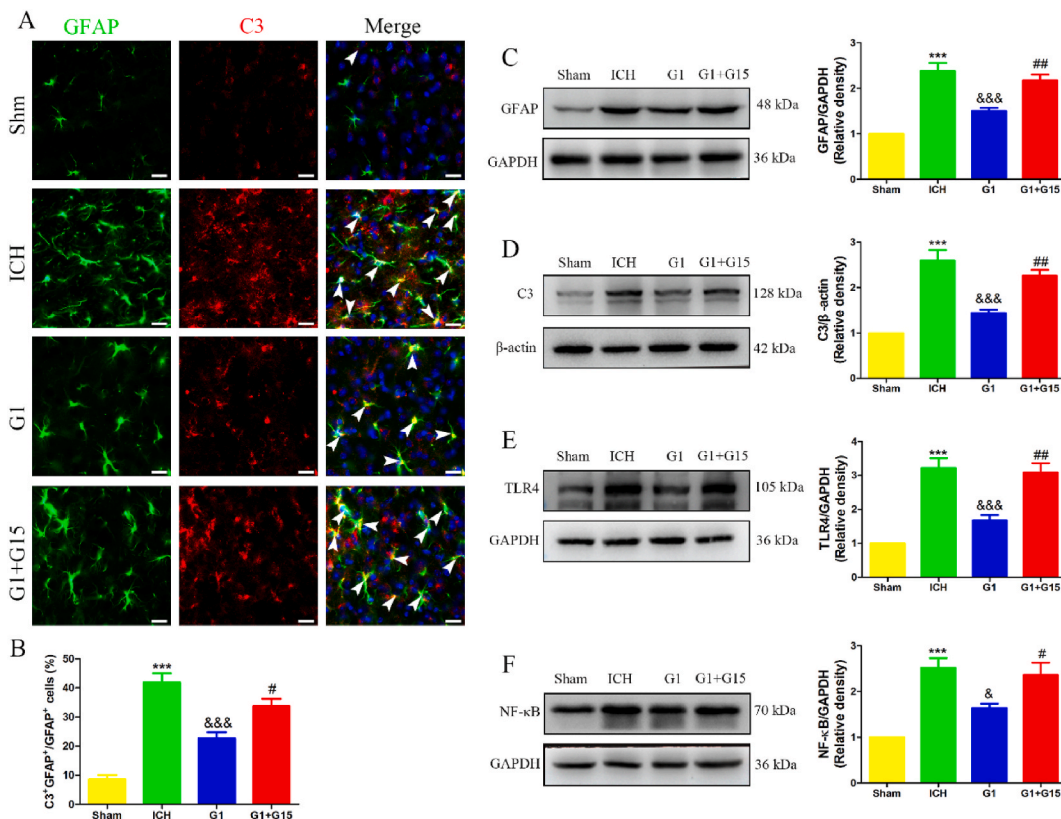


Fig. 6. G15 reduced the inhibitory effect of G1 on A1 reactive astrocytes activation in ICH mice. (A) Representative images of GFAP (green) and complement C3 (red) positive cells in perihematoma tissues on day 3 after ICH. White arrows indicated the A1 astrocytes. (B) Quantitative analysis of GFAP and C3 positive cells in the perihematoma tissues on day 3 after ICH. (C) Representative bands and quantitative analysis of GFAP in the perihematoma area on day 3 after ICH, GAPDH as a loading control. (D) Representative bands and quantitative analysis of complement C3 in the perihematoma area on day 3 after ICH, β-actin was a loading control. (E) Representative bands and quantitative analysis of TLR4 in the perihematoma area on day 3 after ICH, GAPDH was a loading control. (F) Representative bands and quantitative analysis of NF-κB in the perihematoma area on day 3 after ICH, GAPDH was a loading control. n = 4 in each group, ***p < 0.001 vs Sham group, &p < 0.05 vs ICH group, &&p < 0.001 vs ICH group, #p < 0.05 vs G1 group, ##p < 0.01 vs G1 group. Scale bar: 50 μm.

3.5. GPER1 knockout reversed the effect of G1 on inhibition of A1 reactive astrocytes

We further explored the effect of GPER1 on the activation of A1 reactive astrocytes in ICH mice by using GPER1 KO mice. Similar with above data, immunofluorescence staining demonstrated in WT mice, on the day 3 after ICH, G1 significantly reduced the activation of A1 reactive astrocytes, showed as the reduced GFAP and C3 positive cells (20.2 ± 1.281 vs $36 \pm 2.646\%$, $p < 0.01$, Fig. 7A and B). Nevertheless, in GPER1 KO mice, after ICH, G1 did not affected the activation of A1 reactive astrocytes (38 ± 3.209 vs $39 \pm 3.178\%$, $p > 0.05$, Fig. 7A and B). And, G1 markedly decreased the activation of A1 reactive astrocytes in WT mice compared with GPER1 KO mice after ICH (20.2 ± 1.281 vs $38 \pm 3.209\%$, $p < 0.01$, Fig. 7A and B). The semi-quantification analysis of GFAP and C3 indicated, G1 significantly reduced the expression of GFAP (0.5344 ± 0.05712 vs 1 folds, $p < 0.001$) and C3 (0.4538 ± 0.03956 vs 1 folds, $p < 0.001$) in WT mice (Fig. 7C–E). However, G1 did not reduced the expression of GFAP and C3 in GPER1 KO mice ($p > 0.05$, Fig. 7C–E). And, G1 reduced the expression of GFAP (0.5344 ± 0.05712 vs 1.107 ± 0.04149 folds, $p < 0.001$) and C3 (0.4538 ± 0.03956 vs 1.306 ± 0.04251 folds, $p < 0.001$) after ICH in WT mice compared to GPER1 KO mice (Fig. 7C–E). These data further confirmed activation of GPER1 was crucial for inhibiting the activation of A1 reactive astrocytes after ICH.

3.6. TLR4/NF-κB pathway mediated the effect of GPER1 on the activation of A1 reactive astrocytes in ICH mice

Toll-like receptor 4 (TLR4) is a member of Toll-like receptor family and increasing evidences suggest TLR4 is associated with the regulation of inflammation response and astrocytes activation post-stroke [16,28,29]. Then, we detected the expression of TLR4 after

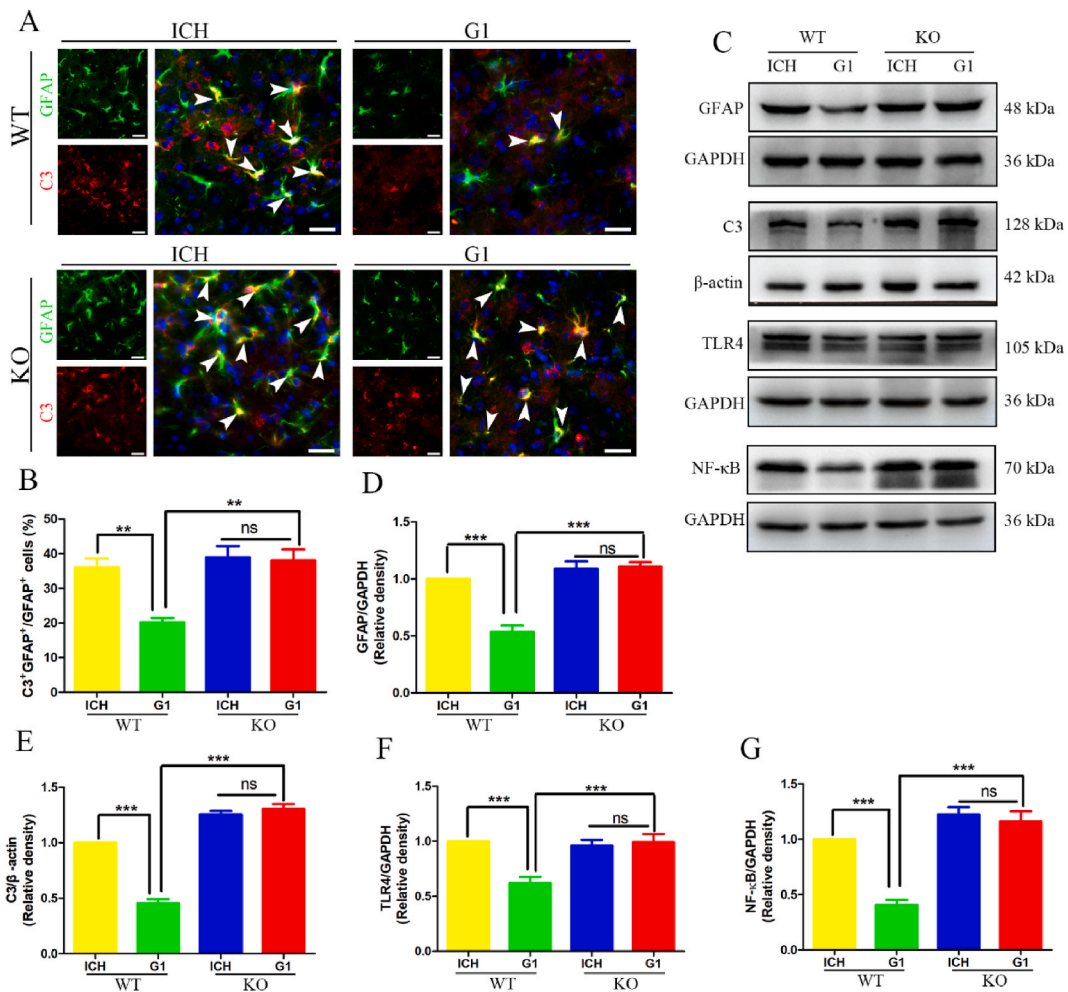


Fig. 7. Knockout GPER1 reversed the inhibition of G1 on A1 reactive astrocytes activation in ICH mice. (A) Representative images of GFAP (green) and complement C3 (red) positive cells in perihematoma tissues on day 3 after ICH. White arrows indicated the A1 astrocytes. (B) Quantitative analysis of GFAP and C3 positive cells in the perihematoma tissues on day 3 after ICH. (C) Representative protein bands of GFAP, complement C3, TLR4, NF-κB in the perihematoma area on day 3 after ICH, and GAPDH or β-actin was a loading control. (D–G) Quantification analysis of GFAP, complement C3, TLR4 and NF-κB in the perihematoma area on day 3 after ICH. n = 4 in each group, **p < 0.01, ***p < 0.001 and ns indicated no significantly difference. Scale bar: 50 μm.

G1 and/or G15 treatment in ICH mice. The results showed TLR4 increased robustly after ICH (3.22 ± 0.2922 vs 1 folds, $p < 0.001$), and G1 decreased the expression of TLR4 compared with ICH group (1.68 ± 0.1562 vs 3.22 ± 0.2922 folds, $p < 0.001$). However, the administration of G15 prevented the down-regulated expression of TLR4 compared to G1 group (3.08 ± 0.2853 vs 1.68 ± 0.1562 folds, $p < 0.01$, Fig. 6E). To further confirm the regulation of TLR4 was mediated by GPER1, the expression of NF- κ B was determined. NF- κ B expression was up-regulated after ICH compared with Sham group (2.52 ± 0.2131 vs 1 folds, $p < 0.001$), and G1 inhibited the up-regulation of NF- κ B compared to ICH + vehicle group (1.64 ± 0.09274 vs 2.52 ± 0.2131 folds, $p < 0.05$). Similarly, G15 abolished the effect of G1 on the regulation of NF- κ B compared to ICH + G1 group (2.36 ± 0.2676 vs 1.64 ± 0.09274 folds, $p < 0.05$, Fig. 6F). In addition, G1 did not significantly down-regulated the expression of TLR4 and NF- κ B compared to ICH group in GPER1 KO mice ($p > 0.05$, Fig. 7C–F, G). However, G1 reduced the expression of TLR4 (0.62 ± 0.05621 vs 0.992 ± 0.07412 folds, $p < 0.001$) and NF- κ B (0.4086 ± 0.04381 vs 1.163 ± 0.0894 folds, $p < 0.001$) in WT mice compared to GPER1 KO mice after ICH (Fig. 7C–F, G), suggesting GPER1 inhibited the activation of A1 reactive astrocytes via down-regulation of TLR4/NF- κ B pathway.

4. Discussions

In the present study, our results indicated that activation of GPER1 improved the neurological function deficits of mice caused by ICH, and reduced the activation of A1 reactive astrocytes in perihematomal region. Meanwhile, down-regulation of TLR4/NF- κ B pathway at least partially mediated the protective effects of GPER1 on the neurological function and inhibition the activation of A1 reactive astrocytes (Fig. 8).

ICH is a catastrophic subtype of stroke. After ICH, inflammatory responses are triggered by the infiltrating of peripheral macrophages and the activation of CNS resident microglia as well as the astrocytes, which participate in the pathophysiological process of EBI in ICH [30–32]. The activation and proliferation of astrocytes after CNS insults have been proved to possess the double-edge sword for CNS damage. On the one hand, activated astrocytes could play a protective effect through restricting injury by the formation of glia scar at acute phase of insult [33]. On the other hand, activated astrocytes have been verified to play a harmful effect via eliciting inflammatory cascade, oxidative stress and glutamate excitotoxicity [34–36]. Emerging evidence shows reactive astrocytes could be polarized to two opposite phenotypes, A1, the neurotoxic type which produce pro-inflammatory factors, and A2, the neuroprotective type, produce anti-inflammatory factors and neurotrophic factors [12,14]. After ICH, the excessive inflammatory responses are contributed to EBI [2,3]. Fei X et al. discovered that the A1 reactive astrocytes activated robustly and peaked on the third day after ICH, and reducing A1 reactive astrocytes by polarized them into A2 reactive astrocytes ameliorated the inflammatory response [20]. Thus, we detected the activation of the A1 reactive astrocytes on the third day after ICH. Our results showed A1 reactive astrocytes were activated rigorously after ICH showed as increased C3⁺GFAP⁺ cells (Figs. 6 and 7).

A large number of studies had proven that estrogen plays multiple important roles in the protection of CNS injury. And estrogen nuclear receptors (including ER α , ER β) as well as membrane estrogen receptor GPER1 mediate the protective effects after CNS injury [23,37,38]. Previous studies demonstrate the novel estrogen receptor GPER1 is essential for the protective effects of estrogen on stroke. The activation of GPER1 reduces the microglia elicited inflammation and alleviates the neurological deficits in ischemic stroke animals [16,24]. And in ischemic stroke, the activation of GPER1 also mediates the BBB protection [39,40]. More than that, GPER1 mediates

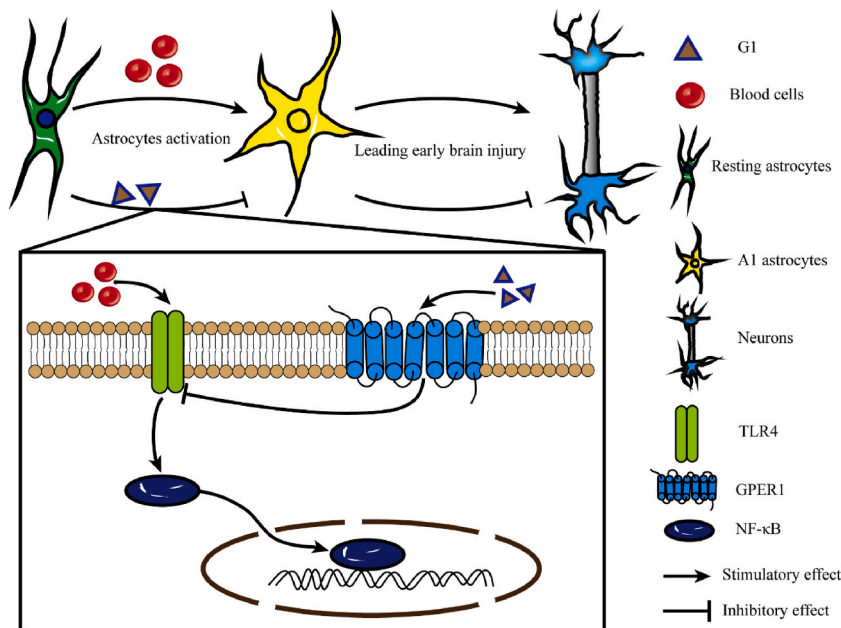


Fig. 8. A schematic illustration for mechanism of activation of GPER1 alleviating EBI by decreasing A1 astrocytes expression after ICH.

the remyelination in cuprizone-induced demyelinate disease [41]. Chen TY et al. found the activation of GPER1 by estrogen could attenuate neurons death through inhibiting autophagy in an iron overloaded model [42]. In addition, GPER1 is involved in the regulation of astrocytes activity in MPTP/MPP⁺ toxic mice model [43]. However, whether GPER1 also protects the neurological function after ICH as well as the potential cellular and molecular mechanism had not been fully clarified. Our data showed activation of GPER1 by G1 after ICH mitigated the EBI reflected as improved neurological deficits (Fig. 2) which is consist with previous study that GPER1 plays a protective effect on CNS damage [22,23,25]. Meanwhile, G1 treatment also decreased the numbers of GFAP positive and C3 positive cells in perihematomal zone (Figs. 3 and 4). Using G15 block GPER1 counteract the effect of G1 on the protection of EBI after ICH (Fig. 5). In addition, the numbers of A1 reactive astrocytes were also increased after G15 treatment or knockout GPER1 (Figs. 6 and 7), indicating inhibition of A1 reactive astrocytes activation may be the cellular mechanism of GPER1 on the protection of EBI after ICH. Considering of the permeability of G1 into BBB, thus, activation of GPER1 by its specific small molecular agonist G1 maybe a promising candidate for the treatment of EBI caused by A1 reactive astrocytes after ICH. The dosage of G1 in experiment I was chosen according to previous reports. In LPS-induced mice nigral inflammation model, 190 µg/kg G1 was able to activate GPER1, and reduce the inflammation-induced nigral dopaminergic loss [22]. And in cuprizone-induced rats demyelination model, 100 µg/kg G1 was also capable of activation of GPER1 [41]. Besides, 300 µg/kg G1 was effective to activation GPER1 in SAH rats [25]. Thus, 100 µg/kg G1 and 200 µg/kg G1 were chosen to test the protective effect of the activation of GPER1 on functional recovery after ICH.

TLR4 is a pathogen recognition receptor in CNS, and TLR4 is expressed in microglia, neurons and astrocytes [44]. And TLR4/NF-κB pathway mediates the excitotoxicity of astrocytes in ICH mice [28]. Previous study in MCAO reveals that the activation of GPER1 in microglia alleviates the inflammatory responses and rescues the neuronal apoptosis in ischemic penumbra via TLR4 [16]. More than that, TLR4/NF-κB pathway mediates the activation of rats astrocytes in vitro ICH model [29]. Our findings demonstrated that the expression level of TLR4 and NF-κB were elevated in perihematomal region after ICH, which is in line with previous studies [28,45,46]. Intriguingly, the activation of GPER1 reversed the increased expression of TLR4 and NF-κB caused by ICH. More importantly, GPER1 knockout abolished the effect of G1 on the upregulated expression of TLR4 and NF-κB (Figs. 6 and 7), suggesting TLR4/NF-κB pathway mediated the inhibitory effect of GPER1 on the activation of A1 reactive astrocytes after ICH, at least in part. In this study we focused the effect of GPER1 on the protection of EBI, and the effect of GPER1 on the activation of A1 reactive astrocytes after ICH. And due to the cross-talk between astrocytes and microglia in producing and exacerbating inflammatory responses, the role of GPER1 on the regulation of microglia activation is not detected which is a limitation of this study. More studies are needed to further clarify the role of GPER1 on the regulation of microglia and A2 astrocytes after ICH. And lack of the in-vitro experiments to investigate the mechanism of GPER1 on the modulation of astrocytes activity is another limitation of this study. More deeply in-vitro experiments are needed to clarify the role of GPER1 on the phenotype transition of astrocytes after ICH.

5. Conclusions

In conclusion, our findings provided evidence that activation of GPER1 mitigates the EBI through inhibiting the activation of A1 reactive astrocytes in perihematomal zone after ICH. Moreover, TLR4/NF-κB pathway mediates the role of GPER1 regulating the activation of A1 reactive astrocytes after ICH. This study provides a perspective that GPER1 maybe as a new candidate target for therapy the inflammatory injury leading EBI caused by A1 reactive astrocytes in ICH patients, and provides a rationale for targeting GPER1 in the treatment of ICH.

Funding statement

Present study was funded by the grants from National Natural Science Foundation of China (82001321, 81972361 and 82271424), and Natural Science Foundation Project of Chongqing, Chongqing Science and Technology Commission, China (cstc2021jcyj-msxmX0631).

Ethics statement

The animal experimental procedures were supervised by the China Animal Welfare Legislation with the approval of the Animal Ethics Committee of Third Military Medical University (Approval ID: SYXK (Yu) 20170002).

Data availability statement

The data will be available from the corresponding author upon reasonable request.

CRedit authorship contribution statement

Jianchao Mao: Writing – original draft, Methodology, Investigation. **Yongkun Guo:** Software, Formal analysis, Data curation. **Huanhuan Li:** Methodology. **Hongfei Ge:** Investigation, Funding acquisition. **Chao Zhang:** Data curation. **Hua Feng:** Supervision, Resources. **Jun Zhong:** Funding acquisition, Conceptualization. **Rong Hu:** Writing – review & editing, Conceptualization. **Xinjun Wang:** Supervision, Funding acquisition, Conceptualization.

Declaration of competing interest

The authors declare that they have no known competing financial interests or personal relationships that could have appeared to influence the work reported in this paper.

Appendix A. Supplementary data

Supplementary data to this article can be found online at <https://doi.org/10.1016/j.heliyon.2024.e26909>.

References

- [1] G.B.D.S. Collaborators, Global, regional, and national burden of stroke and its risk factors, 1990-2019: a systematic analysis for the Global Burden of Disease Study 2019, *Lancet Neurol.* 20 (10) (2021) 795–820.
- [2] D.A. Wilkinson, et al., Injury mechanisms in acute intracerebral hemorrhage, *Neuropharmacology* 134 (Pt B) (2018) 240–248.
- [3] W. Bautista, et al., Secondary mechanisms of injury and viable pathophysiological targets in intracerebral hemorrhage, *Ther Adv Neurol Disord* 14 (2021) 17562864211049208.
- [4] S.N. Ohashi, et al., Role of inflammatory processes in hemorrhagic stroke, *Stroke* 54 (2) (2023) 605–619.
- [5] B.-W. Zhang, et al., The crosstalk between immune cells after intracerebral hemorrhage, *Neuroscience* 537 (2024) 93–104.
- [6] L. Li, et al., A cannabinoid receptor 2 agonist reduces blood-brain barrier damage via induction of MKP-1 after intracerebral hemorrhage in rats, *Brain Res.* 1697 (2018) 113–123.
- [7] L. Lin, et al., Inflammatory regulation by driving microglial M2 polarization: neuroprotective effects of cannabinoid receptor-2 activation in intracerebral hemorrhage, *Front. Immunol.* 8 (2017) 112.
- [8] J. Zeng, et al., Puerarin attenuates intracerebral hemorrhage-induced early brain injury possibly by PI3K/Akt signal activation-mediated suppression of NF- κ B pathway, *J. Cell Mol. Med.* 25 (16) (2021) 7809–7824.
- [9] M. Chen, et al., LZK-dependent stimulation of astrocyte reactivity promotes corticospinal axon sprouting, *Front. Cell. Neurosci.* 16 (2022) 969261.
- [10] Z. Ma, et al., Neuromodulators signal through astrocytes to alter neural circuit activity and behaviour, *Nature* 539 (7629) (2016) 428–432.
- [11] S.D. Verma, et al., Astrocytes regulate vascular endothelial responses to simulated deep space radiation in a human organ-on-a-chip model, *Front. Immunol.* 13 (2022) 864923.
- [12] S.A. Liddelow, B.A. Barres, Reactive astrocytes: production, function, and therapeutic potential, *Immunity* 46 (6) (2017) 957–967.
- [13] F. Khodadadei, et al., The effect of A1 and A2 reactive astrocyte expression on hydrocephalus shunt failure, *Fluids Barriers CNS* 19 (1) (2022) 78.
- [14] S.A. Liddelow, et al., Neurotoxic reactive astrocytes are induced by activated microglia, *Nature* 541 (7638) (2017) 481–487.
- [15] D.M. Taha, et al., Astrocytes display cell autonomous and diverse early reactive states in familial amyotrophic lateral sclerosis, *Brain* 145 (2) (2022) 481–489.
- [16] Z. Zhang, et al., The novel estrogenic receptor GPR30 alleviates ischemic injury by inhibiting TLR4-mediated microglial inflammation, *J. Neuroinflammation* 15 (1) (2018) 206.
- [17] H.J. Zou, et al., Methylprednisolone induces neuro-protective effects via the inhibition of A1 astrocyte activation in traumatic spinal cord injury mouse models, *Front. Neurosci.* 15 (2021) 628917.
- [18] P. An, et al., Dexmedetomidine alleviates intracerebral hemorrhage-induced anxiety-like behaviors in mice through the inhibition of TRPV4 opening, *Front. Pharmacol.* 13 (2022) 852401.
- [19] J. Zheng, et al., Ceria nanoparticles ameliorate white matter injury after intracerebral hemorrhage: microglia-astrocyte involvement in remyelination, *J. Neuroinflammation* 18 (1) (2021) 43.
- [20] X. Fei, et al., Homer1 promotes the conversion of A1 astrocytes to A2 astrocytes and improves the recovery of transgenic mice after intracerebral hemorrhage, *J. Neuroinflammation* 19 (1) (2022) 67.
- [21] A. Alexander, A.J. Irving, J. Harvey, Emerging roles for the novel estrogen-sensing receptor GPER1 in the CNS, *Neuropharmacology* 113 (Pt B) (2017) 652–660.
- [22] J. Mendes-Oliveira, et al., GPER activation is effective in protecting against inflammation-induced nigral dopaminergic loss and motor function impairment, *Brain Behav. Immun.* 64 (2017) 296–307.
- [23] S. Wang, et al., Neuronal GPER participates in genistein-mediated neuroprotection in ischemic stroke by inhibiting NLRP3 inflammasome activation in ovariectomized female mice, *Mol. Neurobiol.* 59 (8) (2022) 5024–5040.
- [24] T.Z. Zhao, et al., GPER expressed on microglia mediates the anti-inflammatory effect of estradiol in ischemic stroke, *Brain and Behavior* 6 (4) (2016).
- [25] J. Peng, et al., Activation of GPR30 with G1 attenuates neuronal apoptosis via src/EGFR/stat3 signaling pathway after subarachnoid hemorrhage in male rats, *Exp. Neurol.* 320 (2019) 113008.
- [26] X.S. Wang, et al., Activation of G protein-coupled receptor 30 protects neurons by regulating autophagy in astrocytes, *Glia* 68 (1) (2020) 27–43.
- [27] B. Wang, et al., Dextramipexole attenuates white matter injury to facilitate locomotion and motor coordination recovery via reducing ferroptosis after intracerebral hemorrhage, *Oxid. Med. Cell. Longev.* 2022 (2022) 6160701.
- [28] J. Xu, et al., Potential anti-inflammatory effect of anti-HMGB1 in animal models of ICH by downregulating the TLR4 signaling pathway and regulating the inflammatory cytokines along with increasing HO1 and NRF2, *Eur. J. Pharmacol.* 915 (2022) 174694.
- [29] S. Deng, et al., AQP2 promotes astrocyte activation by modulating the TLR4/NF κ B-p65 pathway following intracerebral hemorrhage, *Front. Immunol.* 13 (2022) 847360.
- [30] X. Hu, et al., Oxidative Stress in Intracerebral Hemorrhage: Sources, Mechanisms, and Therapeutic Targets, vol. 2016, *Oxid Med Cell Longev.* 2016 3215391.
- [31] S. Chen, et al., An update on inflammation in the acute phase of intracerebral hemorrhage, *Transl Stroke Res* 6 (1) (2015) 4–8.
- [32] J.W.a.S. Doré, Heme oxygenase-1 exacerbates early brain injury after intracerebral haemorrhage, *Brain* 130 (6) (2007) 1643–1652 (pt).
- [33] Y. Yuan, et al., p-hydroxy benzaldehyde revitalizes the microenvironment of peri-infarct cortex in rats after cerebral ischemia-reperfusion, *Phytomedicine* 105 (2022) 154379.
- [34] J. Companys-Aleman, et al., Glial cell reactivity and oxidative stress prevention in Alzheimer's disease mice model by an optimized NMDA receptor antagonist, *Sci. Rep.* 12 (1) (2022) 17908.
- [35] E. Pajarillo, et al., Astrocytic Yin Yang 1 is critical for murine brain development and protection against apoptosis, oxidative stress, and inflammation, *Glia* 71 (2) (2022) 450–466.
- [36] J. Zhou, et al., Suppression of NDRG2 alleviates brain injury after intracerebral hemorrhage through mitigating astrocyte-driven glutamate neurotoxicity via NF- κ B/GLT1 signaling, *Brain Res.* 1729 (2020) 146600.
- [37] J.Z. Hu, et al., The effect of estrogen-related receptor alpha on the regulation of angiogenesis after spinal cord injury, *Neuroscience* 290 (2015) 570–580.
- [38] S. Lee, et al., Estrogen receptor-beta of microglia underlies sexual differentiation of neuronal protection via ginsenosides in mice brain, *CNS Neurosci. Ther.* 24 (10) (2018) 930–939.
- [39] T. Murata, et al., G protein-coupled estrogen receptor agonist improves cerebral microvascular function after hypoxia/reoxygenation injury in male and female rats, *Stroke* 44 (3) (2013) 779–785.

- [40] D. Lu, et al., Activation of G protein-coupled estrogen receptor 1 (GPER-1) ameliorates blood-brain barrier permeability after global cerebral ischemia in ovariectomized rats, *Biochem. Biophys. Res. Commun.* 477 (2) (2016) 209–214.
- [41] Y. Hirahara, et al., G protein-coupled receptor 30 contributes to improved remyelination after cuprizone-induced demyelination, *Glia* 61 (3) (2013) 420–431.
- [42] T.Y. Chen, et al., Targeting GPER1 to suppress autophagy as a male-specific therapeutic strategy for iron-induced striatal injury, *Sci. Rep.* 9 (1) (2019) 6661.
- [43] L.J. Yuan, et al., Anti-inflammatory effect of IGF-1 is mediated by IGF-1R cross talk with GPER in MPTP/MPP(+)-induced astrocyte activation, *Mol. Cell. Endocrinol.* 519 (2021) 111053.
- [44] S. Takahashi, K. Mashima, Neuroprotection and disease modification by astrocytes and microglia in Parkinson disease, *Antioxidants* 11 (1) (2022).
- [45] S. Liu, et al., TREM2 improves neurological dysfunction and attenuates neuroinflammation, TLR signaling and neuronal apoptosis in the acute phase of intracerebral hemorrhage, *Front. Aging Neurosci.* 14 (2022).
- [46] Y. Yang, et al., Luteolin alleviates neuroinflammation via downregulating the TLR4/TRAF6/NF- κ B pathway after intracerebral hemorrhage, *Biomed. Pharmacother.* 126 (2020) 110044.